

Received March 16, 2021, accepted May 2, 2021, date of publication May 10, 2021, date of current version May 19, 2021.

Digital Object Identifier 10.1109/ACCESS.2021.3078554

Neural Network Model for Magnetization Characteristics of Ferromagnetic Materials

MINGXING TIAN^{1,2}, HONGCHEN LI¹, AND HUIYING ZHANG^{1,2}

¹School of Automation and Electrical Engineering, Lanzhou Jiaotong University, Lanzhou 730070, China

²Rail Transit Electrical Automation Engineering Laboratory of Gansu Province, Lanzhou Jiaotong University, Lanzhou 730070, China

Corresponding author: Mingxing Tian (tianmingxing@mail.lzjtu.cn)

This work was supported in part by the Science and Technology Program of Gansu Province, China, under Grant 17JR5RA083, in part by the National Natural Science Foundation of China under Grant 51867012 and Grant 51367010, and in part by the Program for Excellent Team of Scientific Research in Lanzhou Jiaotong University, China, under Grant 201701.

ABSTRACT The magnetic characteristics of silicon steel sheet 30Q120 under different AC frequencies were measured by an Epstein frame in order to analyze the effects of frequency variation on the hysteresis loop of ferromagnetic materials and compare the differences of such materials at different frequencies. First, the forecasting method of the magnetic properties of ferromagnetic materials under the influence of frequency using neural network was proposed based on the measured experimental data. Hysteresis loops at different frequencies were obtained. Then, the obtained results were compared with the measured results. Second, the dynamic Jiles–Atherton hysteresis model was established based on the Jiles–Atherton hysteresis theory, and hysteresis loops at different frequencies were obtained. The accuracies of the neural network model and Jiles–Atherton hysteresis model were verified by comparing the simulation results with the measured data. Upon comparing the dynamic Jiles–Atherton hysteresis and the neural network hysteresis models, results show that the latter has better accuracy. Furthermore, the correctness and effectiveness of the proposed method are verified.

INDEX TERMS Dynamic Jiles–Atherton model, frequency, ferromagnetic materials, hysteresis loop, neural network.

I. INTRODUCTION

Transformers, reactors, and motors, among others, are important electromagnetic equipment in a power system. Studies on the magnetic characteristics of the core of such a system present important content by which to analyze the operation of electromagnetic equipment. Furthermore, the accurate establishment of a ferromagnetic core magnetization model is critical in the analysis of electromagnetic equipment. The saturation and hysteresis nonlinearity of core magnetization greatly increase the difficulty of core modeling and analysis. In order to establish such a model, the partial magnetization model abandons the consideration of hysteresis characteristics and nonlinearity and, instead, uses simple linear condition. Although the modeling process is simplified, there is a large error in the accuracy of the model, which cannot completely simulate the magnetic characteristics of the iron core. In addition, considering the nonlinear relationship makes the modeling more difficult. Therefore, selecting a

suitable magnetization model, which can not only guarantee the modeling accuracy but also realize the modeling of the core in a simple and efficient way, is very important.

Due to the complex and changeable working environment of electromagnetic equipment, coupled with the influences of frequency, temperature, DC (harmonic) magnetic bias, core shape, core lamination stress and other factors, the core magnetic characteristics will change, subsequently affecting the normal operation of the electromagnetic equipment. The need for the accurate description of dynamic magnetization curves under arbitrary magnetization conditions resulted in the development of various models. Conventional hysteresis models, such as Jiles–Atherton (J–A) model [1] and Preisach model [2], are widely used in the study of hysteresis loops because of their relatively stable characteristics and good computational performance. Scholars tend to compare different hysteresis models in the in-depth study of loss and hysteresis. Appropriate models are selected by analyzing the advantages and limitations of different models [3], [4], and new forms are derived from classical models to form class models [5], [6]. The most suitable model is found by

The associate editor coordinating the review of this manuscript and approving it for publication was Seyedali Mirjalili.

comparing the results of different models. However, a model still cannot avoid parameter identification and is constrained by accuracy and simplicity. The model and experimental results have a big gap when distorted and irregular hysteresis loops are encountered [7]. In order to study the influence of the above factors on the core, many researchers have improved the model, establishing the hysteresis model by considering some factors and introducing the parameters to express the relevant factors. Hysteresis models were established in [8], [9] wherein temperature change was represented by using the Preisach and J–A models, respectively, after which the authors analyzed the effects of temperature change on the hysteresis loop. A new parameter identification method was proposed for the Preisach model in [10], which established the dynamic hysteresis model under DC bias and analyzed the influence of DC bias on the loss, but the process of generating the first order reversal curve is complicated. The magnetic characteristics of DC bias at different frequencies of 50 and 100 Hz were simulated and analyzed in [11], but the modeling process was complex and the workload was too heavy. The influence of frequency on the magnetic properties of electrical steel was studied by measuring the magnetic properties of electrical steel at different frequencies in [12], [13], but the relevant magnetization model of ferromagnetic materials was not established. The application of the model under the influence of many factors is limited, because there are few factors that affect the magnetic characteristics in modeling.

In recent years, researchers have paid increasing attention to the continuous development of neural network for ferromagnetic materials magnetization model due to its good non-linear processing ability [14]–[16]. First, compared with the common J–A and Preisach models, the relationship between magnetic field strength H and magnetic flux density B can be directly obtained by the magnetization neural network model, thus simplifying the modeling process. Second, the neural network model of magnetic characteristics does not need to introduce parameters when establishing the magnetization model affected by some factors. This not only reduces the complexity of the model, but also avoids the tedious calculation of model parameters. Furthermore, to take a certain factor into account, it is only necessary to add a neuron input representing the factor in the input layer of the neural network. Therefore, the neural network can consider multiple factors at the same time.

The method that by using neural network to solve the complex modeling problem of DC magnetic bias was proposed to simulate hysteresis loop under DC magnetic bias in [17]. In the existing literature on the use of neural networks, no neural network hysteresis model considering frequency alone has been found.

The study of magnetic properties at different frequencies helps in identifying the methods that can be used to reduce the loss and those that can obtain the suitable working frequency ranges of different types of silicon steel sheets, thus providing an important basis for the reasonable selection of

ferromagnetic materials in different frequency ranges. Therefore, based on the measurement of the magnetic properties of silicon steel sheet at different frequencies, a neural network hysteresis model that considers frequency is proposed in this paper to study the differences in the magnetic properties of ferromagnetic materials at different frequencies. The results of the neural network prediction, dynamic J–A model, and experimental measurement are compared. The comparison results prove the accuracy of the proposed neural network model.

II. DYNAMIC JILES-ATHERTON HYSTERESIS MODEL

The J–A model is a typical representative of the second type of theoretical model, which has a relatively simple expression and clear physical meaning. This model has been widely used in the modeling of the excitation characteristics of magnetic materials. J–A model is based on the energy-balance equation. It is relatively simple and involves the computation of only five parameters. The anhysteretic magnetization is expressed as

$$M_{an} = M_s \left[\coth\left(\frac{H_e}{a}\right) - \frac{a}{H_e} \right] \quad (1)$$

where M_{an} is the anhysteretic magnetization, M_s is the saturation magnetization, and a is the loop shape parameter, in addition, H_e is the effective field, which can be written as

$$H_e = H + \alpha M \quad (2)$$

where H is applied magnetic field, α is the interdomain coupling parameter, and M is the total magnetization.

The dynamic loss term can be written as [18]

$$P(t) = k_e \left| \frac{dB}{dt} \right| + k_a \left(\left| \frac{dB}{dt} \right| \right)^{\frac{1}{2}} \quad (3)$$

where k_a and k_e are the dynamic loss parameter, and B is magnetic flux density. The differential expression of the inverse J–A hysteresis model is expressed as

$$\frac{dM}{dB} = \frac{\delta_M(M - M_{an}) - k\delta c \frac{dM_{an}}{dH_e}}{\mu_0 \left[(1-\alpha)\delta_M(M_{an} - M) - k\delta c \frac{dM_{an}}{dH_e} - k\delta - P_d(t) \right]} \quad (4)$$

where δ_M is used to avoid unphysical solutions, $\delta_M = 0.5[1 + \text{sign}(M_{an} - M) \frac{dB}{dt}]$, μ_0 is the magnetic permeability of free space, k is the pinning parameter, c is a reversibility parameter, and δ is a directional parameter having the value +1 for $dB/dt > 0$ and -1 for $dB/dt < 0$.

The detailed expression of the dynamic inverse J–A model is described in (5) below [19].

$$\begin{aligned} & \frac{dM}{dB} \\ &= \frac{\delta_M(1-c)(M_{an} - M) + k\delta c \frac{dM_{an}}{dH} - (1-c)(k_e \frac{dB}{dt} - k_a \delta \left| \frac{dB}{dt} \right|^{\frac{1}{2}})}{\mu_0 \delta_M(1-c)(1-\alpha)(M_{an} - M) + \mu_0 k \delta + \mu_0 k \delta c \frac{dM_{an}}{dH}} \end{aligned} \quad (5)$$

III. NEURAL NETWORK HYSTERESIS MOEDL

Back propagation (BP) neural network is a neural network that utilizes error BP learning algorithm to change weights and thresholds through feedback value [20]. In BP neural network, variables have no fixed mathematical relationship as determined by learning the given examples in the training process. The model can summarize the correct answers, which are similar to the data given in the training stage. Robert Hecht Nielsen proved in 1989 that a BP neural network with hidden layers can approximate continuous functions in any closed interval. In other words, any mapping from the n -dimension to the m -dimension can be realized by a three-layer BP neural network [21], [22]. Therefore, in order to meet the accuracy requirement of the neural network while avoiding network complexity due to the excessive number of hidden layers, this paper selects a three-layer BP neural network with one hidden layer.

The hysteresis loop aims to achieve a corresponding magnetic field strength value H through a neural network under a given magnetic flux density value B [23]. Given that the magnetic field intensity and magnetic flux density do not have a one-to-one correspondence, in order to better predict the hysteresis loop and prevent the model from being complicated due to the overall prediction of this loop, the hysteresis loop is divided into ascending and descending branches, which are represented by shape coefficient s . When $s = 1$, it represents the process of increasing magnetic field strength, namely, rising branch; when $s = -1$, it indicates the decreasing process of magnetic field strength, that is, the descending branch. Under a certain magnetization condition, the hysteresis loop of ferromagnetic material is determined, and the maximum of the magnetic flux density B_m and the maximum of the magnetic field strength H_m of such a loop are also determined. When the B_m and different B and s of a hysteresis loop are known, the corresponding hysteresis loop can be determined. Therefore, when the magnetic induction strength B is changed, the corresponding magnetic field strength H will be obtained. To study the magnetic properties at different frequencies, frequency f is also used as input [16], [24]. Consequently, a four-input and single-output backpropagation (BP) neural network was built to simulate the hysteresis properties of ferromagnetic materials. The input layer has four neurons. B_m , B , f , and s were the inputs, and the magnetic field strength H was the output, as shown in Fig. 1.

The hysteresis model of the BP neural network shown in Fig. 1 can be represented by the mapping relationship shown in (6).

$$H = f(B_m, B, f, s) \quad (6)$$

where B_m is the maximum of the magnetic flux density, B is the magnetic flux density, s is the shape coefficient and a factor reflecting whether the hysteresis loop is going through the ascending phase or descending phase, f is the magnetization frequency, H is the magnetic field strength.

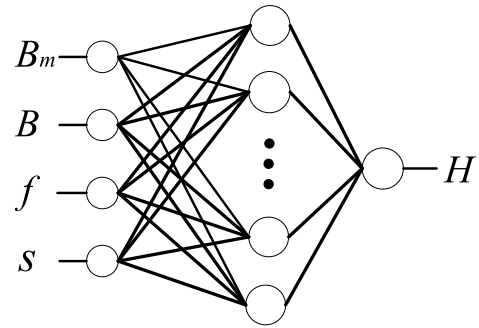


FIGURE 1. Hysteresis model of the BP neural network.

IV. HYSTERESIS LOOP MEASUREMENT

A MATS-3000M/K200 silicon steel material measuring device is selected as the experimental equipment. This device is a standard magnetic measurement equipment based on calculator, software A/D data acquisition, and ARM embedded system. The AC magnetic parameters of soft materials, such as electrical steel sheet (strip), permalloy, amorphous, and nanocrystalline in the frequency range of 20 Hz-2 kHz can be accurately measured, including specific total loss, magnetic polarization strength, magnetic field strength, specific apparent power, maximum permeability, AC magnetization curve and loss curve. The system design meets the requirements of IEC6040-6, IEC6040-3, IEC60404-2, GB/T3655-2008, GB/T13789-2008, GB/T3658-2008, GB/T19346.1-2017, and other standards and specifications.

The 30q120 silicon steel sheet with the specification of 30 mm × 3 mm × 0.3 mm and material density of 7650 kg/m³ was used in the experiment. For B_m , the corresponding value of the saturation hysteresis loop (Bs-Hs) of ferromagnetic material should be selected. However, if the saturation magnetic flux density is too large, it will exceed the measurement range of the experimental device at a certain frequency. Therefore, in order to be able to approach the saturation hysteresis loop of ferromagnetic materials as much as possible, and on the premise that the experimental device can complete the measurement, and within the measurable frequency range selected in this article, the experiment in this paper is finally determined the selected value is 1.8T by continuously adjusting the saturation magnetic flux density value. The magnetic properties of ferromagnetic materials at 25 Hz and 50–550 Hz (50Hz as interval) with B_m of 1.8T were measured experimentally [25], and the corresponding hysteresis loop data were obtained. Each frequency corresponds to a group of data. When measuring points, the system determines the number of sampling points according to the set frequency, and the data pairs in each group of data are obtained. In order to avoid the imbalance of sample data extraction in neural network prediction, 25, 100, 200, 300, 400, and 500 Hz are selected as the training data of neural network at a lower frequency. The corresponding numbers of data pairs under each frequency were 781, 781, 781, 521, 781, and 625. The residual frequency values of 50, 150, 250, 350, 450, and 550 Hz were used as prediction data, and the

numbers of their respective data were 781, 624, 890, 694, and 568 respectively.

V. DETERMINATION OF THE HYSTERESIS MODEL PARAMETERS

A. JILES-ATHERTON MODEL

In order to obtain the parameters in the model, the magnetic properties of silicon steel sheet were measured by using the silicon steel measuring system, thus obtaining many parameters, including the hysteresis loop.

The dynamic J–A hysteresis model has seven parameters, which can be divided into two parts, that is, five are parameters (M_s, α, a, k, c) of the static J–A hysteresis model and two are dynamic loss parameters (k_e, k_a).

Parameter identification was realized by particle intelligent optimization [26]. The static hysteresis loop of 30Q120 silicon steel sheet under direct current was measured with a silicon steel measuring device. Based on the J–A hysteresis model, the static hysteresis model with flux as input was derived using the hysteresis loop. Five parameters were obtained by discrete integration and incorporated into the static J–A model to obtain the B–H curve and calculate magnetic field strength. The root mean square error between the measured and calculated values was obtained by (7) as the objective function of the algorithm to continuously adjust the five parameters of the static model. The five parameters identified by static hysteresis loop were obtained when the error met the set value.

$$Fit = \sqrt{\frac{\sum_{i=1}^n (H_{mea}(i) - H_{cal}(i))^2}{n}} \tag{7}$$

where H_{mea} is the experimental measurement of magnetic field strength, H_{cal} is the calculated magnetic field strength, n is the number of samples.

According to the theory of core loss separation, the core loss can be divided into three parts [27]

$$W = W_h + W_e + W_a \tag{8}$$

where W is the core loss, W_h is the hysteresis loss, W_e is eddy current loss, W_a is anomalous loss.

For the frequency dependent eddy current loss and anomalous loss, the expression of W_e per unit volume is

$$W_e = k_e \int_0^T \left(\frac{dB}{dt}\right)^2 dt \tag{9}$$

the expression of W_a per unit volume is

$$W_a = k_a \int_0^T \left(\frac{dB}{dt}\right)^{\frac{3}{2}} dt \tag{10}$$

Dynamic loss has a greater influence on the core loss with the increase in frequency. Therefore, dynamic loss cannot be ignored. In this paper, the hysteresis loops at 50 and 100 Hz were measured, and their core losses expressed as W_1 and W_2 , respectively, were obtained by integrating them. Hysteresis loss W_h can be obtained by calculating the area of the static

hysteresis loop. Dynamic loss coefficient can be obtained based on the following equation (11).

The model parameters were as follows: $c = 2.032 \times 10^{-3}$, $k = 20.1$ A/m, $a = 1.5$ A/m, $\alpha = 3.096 \times 10^{-6}$, $M_s = 1440450$ A/m. The dynamic loss coefficients: $k_a = 0.337$, $k_e = 0.0135$. The hysteresis loop of 1.8T magnetic induction and frequency of 50 Hz is calculated by using the dynamic J–A model, and the experimental measured value is compared with the calculated value, as shown in Fig. 2.

$$\begin{bmatrix} k_e \\ k_a \end{bmatrix} = \begin{bmatrix} \int_0^{T_1} \frac{dB}{dt} dB \int_0^{T_1} \lambda \left| \frac{dB}{dt} \right|^{\frac{1}{2}} dB \\ \int_0^{T_2} \frac{dB}{dt} dB \int_0^{T_2} \lambda \left| \frac{dB}{dt} \right|^{\frac{1}{2}} dB \end{bmatrix}^{-1} \cdot \begin{bmatrix} W_1 - W_h \\ W_2 - W_h \end{bmatrix} \tag{11}$$

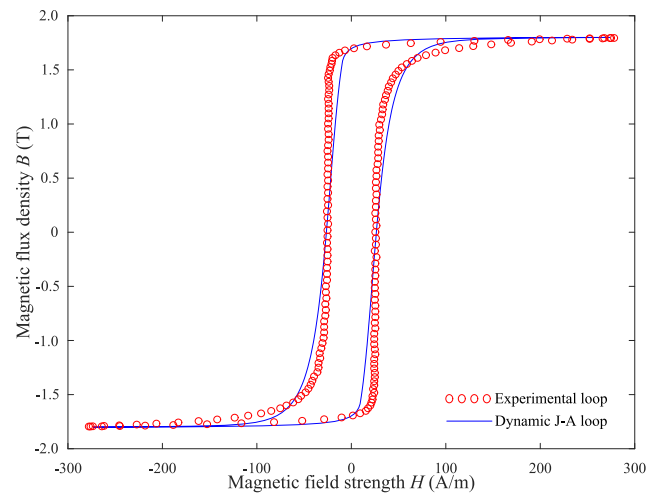


FIGURE 2. Comparison of the J-A model calculation and experimental measurement.

where T_1, T_2 are the corresponding periods at 50 Hz and 100 Hz respectively, λ is the sign coefficient,

$$\lambda = \text{sign}(dB/dt).$$

We can obtain from the Fig. 2 that the measured hysteresis loops are in good agreement with those calculated by dynamic J–A model. The maximum of the magnetic field strength H_m , the maximum of the magnetic flux density B_m , and coercivity H_c of the two results are basically consistent. When the hysteresis loop is close to B_r , the value of the J–A model changes faster than that of the real side. Overall, the results obtained by the J–A model are basically consistent with the measured results and indicate the rationality of the dynamic model and the accuracy of parameter identification.

B. NEURAL NETWORK MODEL

Because the fact that the measured hysteresis loop data are numerous and the numerical range is scattered, a great difference exists between the inputs of the neural network. The numerical problems caused by the inconsistency of the

inputs' orders of magnitude must be avoided, and the larger value must be prevented from affecting the global adjustment of weights and thresholds, thus resulting in a neural network obtaining wrong mapping relationship. Improving the generalization ability of the network and accelerating its convergence speed can better realize the prediction of the neural network. The training data and test data were normalized respectively by using (12),

$$y = \frac{2 * (x - x_{\min})}{(x_{\max} - x_{\min})} \quad (12)$$

where x_{\max} and x_{\min} are the maximum and minimum values of the data respectively; x represents the data before normalization; and y represents the data after normalization. After the prediction is finished, the results are inverse normalized.

The hidden layer node adopts the Sigmoid function, which is continuous and differentiable and has the function of nonlinear amplification coefficient; thus, it is very suitable for nonlinear input and output processing and approximation [29]. When the neural network model in this paper is normalized, the value is between -1 and 1 , and the transfer function of the hidden layer is a tangent transfer function. For the output layer, the output of the neural network model is the magnetic field strength H . Moreover, the range of the magnetic field strength under the saturation magnetic flux density of the hysteresis loop selected in the experiment is relatively large. Therefore, the output value of the network cannot be confined to a very small range. As the transfer function of the output layer, the linear transfer function can be used to realize the output of any value [28].

The number of neurons in each hidden layer are very important in the application of the BP neural network model because they have great influences on the accuracy of the model. The number of neurons in the hidden layer usually depends on the complexity of the problem, as well as on the number of neurons in the input and output layers. However, the empirical formulas for the optimization of the hidden layer are few [30], [31]. First, a certain number of neurons is set, and the network performance is optimized by adjusting the number of neurons. Currently, the number of hidden layer neurons is the final number. In other words, under the requirement of ensuring accuracy, the minimum number of neurons is used to simplify the network structure. The number of nodes in the initial hidden layer is determined by using (13) [32],

$$b = \sqrt{n + l} + a \quad (13)$$

where b is the number of neurons in the hidden layer, n is the number of neurons in the input layer, l is the number of neurons in the output layer, and a is a constant between 1 and 10. By adjusting the number of neurons in the hidden layer, the number of neurons of the hidden layer in this paper is finally determined to be 10.

The network parameters are set as follows: the value of the training goal is 0.00001 and the learning rate is 0.001.

VI. RESULTS AND DISCUSSION

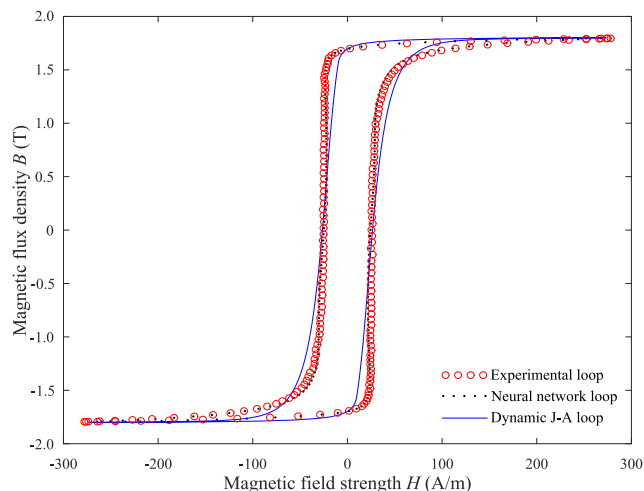
The hysteresis loops at different frequencies are predicted by the neural network based on the experimental data of hysteresis loops, after which the experimental values, neural network predicted values, and dynamic J–A model calculated values are compared. The comparison of the three loops at different frequencies of 50, 150, 250, 350, 450, and 550 Hz is shown in Fig. 3.

We observe from Fig. 3 that, with the increase of frequency, the measured hysteresis loop area of the ferromagnetic materials gradually increases, which is the result of the loss increasing along with the increase of frequency. At different frequencies, the hysteresis loops predicted by the neural network are in good agreement with the experimental ones, and the prediction of special points, such as remanence B_r and coercivity H_c , is ideal. With the increase of frequency, although the shape of the curves on both sides of the hysteresis loop obviously changes, especially from 250 Hz, both sides of the hysteresis loop remain curved. Especially when the curves near the top and the bottom are convex, the hysteresis loop appears as a bulge, but the neural network can still accurately predict these special changes.

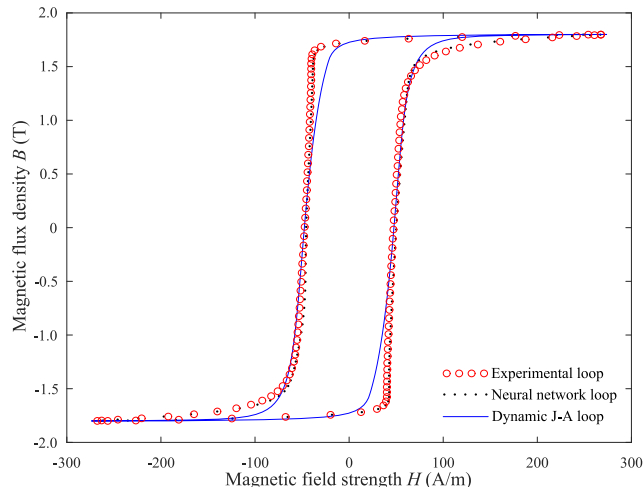
However, the hysteresis loop calculated by the dynamic J–A model is not ideal. It can be seen that at 50, 150, and 250 Hz, the dynamic J–A model is basically consistent with the predicted and measured values of the neural network, and the special points on the hysteresis loop, such as remanence B_r , coercivity H_c , and the maximum of the magnetic field strength H_m , are close to the measured values. However, as the frequency continues to increase, at 350, 450, and 550 Hz, the hysteresis loops obtained by the dynamic J–A model are obviously different from the predicted hysteresis loop and the experimental hysteresis loop. Furthermore, the hysteresis loop area obtained by dynamic J–A model is obviously smaller than that of the other two cases.

As the experimental device can measure B_r and H_c equivalent values at one time, the values obtained by the two methods are compared with the actual measured values, and the errors under the corresponding values are calculated. This is done in order to compare the difference between the results obtained by the neural network model and the dynamic J–A model with the experimental measurements and analyze the accuracy of the two models. The results are shown in Table 1

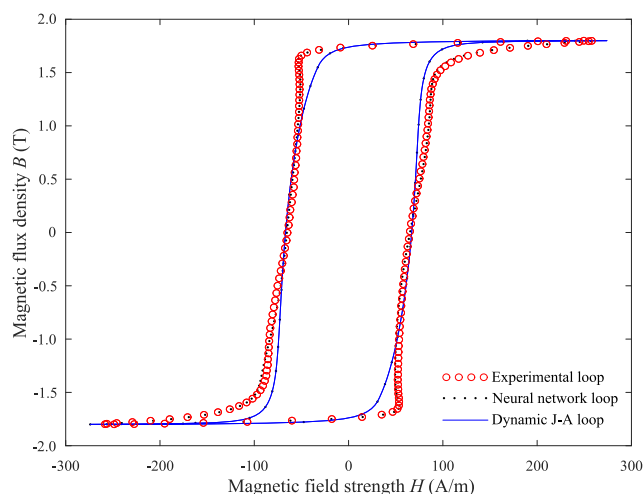
We observe from the data in Table 1 that the frequency increases, the remanence B_r and coercivity H_c increase, the coercivity increment is larger, and the remanence increment is smaller. After comparing the predicted data with the measured data, we find that the prediction results of B_r and H_c of the two models are better, and the error value is acceptable. We observe that the prediction results of the neural network are better than those of the dynamic J–A model in both coercivity and residual flux density. Although the hysteresis loop obtained by the J–A model is less consistent with the measured results than the neural network, the error results of the coercivity and remanence are acceptable.



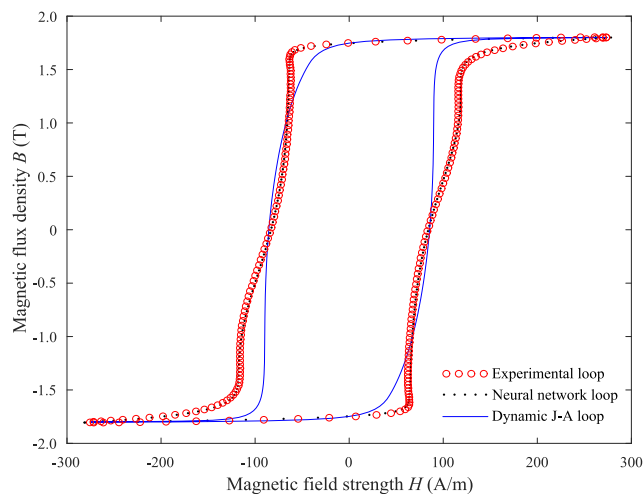
(a) Comparison between the measured result, neural network model, and J-A model when $f = 50$ Hz.



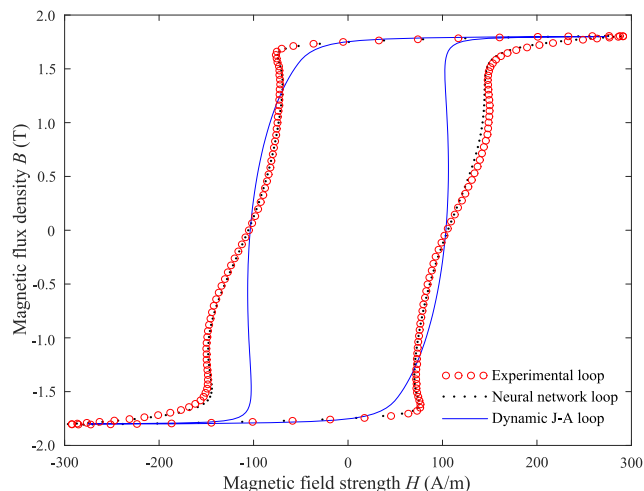
(b) Comparison between the measured result, neural network model, and J-A model when $f = 150$ Hz.



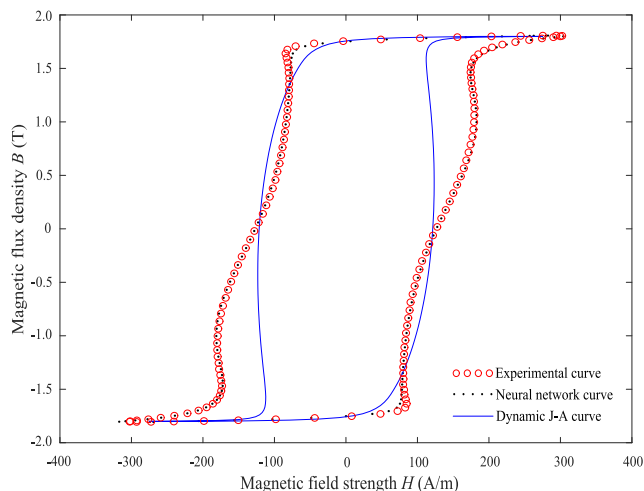
(c) Comparison between the measured result, neural network model, and J-A model when $f = 250$ Hz.



(d) Comparison between the measured result, neural network model, and J-A model when $f = 350$ Hz.



(e) Comparison between the measured result, neural network model, and J-A model when $f = 450$ Hz.



(f) Comparison between the measured result, neural network model, and J-A model when $f = 550$ Hz.

FIGURE 3. Comparison of three results under different frequencies.

TABLE 1. Comparison of the results of the two models and the measured results.

Frequency f (Hz)	Coercivity H_c (A/m)					Remanence B_r (T)				
	Measured value	NN model	Error /%	J-A model	Error /%	Measured value	NN model	Error /%	J-A model	Error /%
50	25.31	25.00	1.24	26.47	-4.58	1.695	1.695	0	1.697	-0.118
150	46.89	45.62	2.70	47.60	-1.51	1.728	1.726	0.116	1.727	0.058
250	64.73	65.53	-1.24	66.91	-3.37	1.738	1.738	0	1.740	-0.115
350	83.60	83.43	0.20	85.46	-2.22	1.750	1.747	0.171	1.743	0.400
450	104.80	104.99	-0.18	103.56	1.18	1.752	1.750	0.114	1.754	-0.114
550	126.20	126.96	-0.06	121.37	3.83	1.754	1.752	0.114	1.758	-0.228

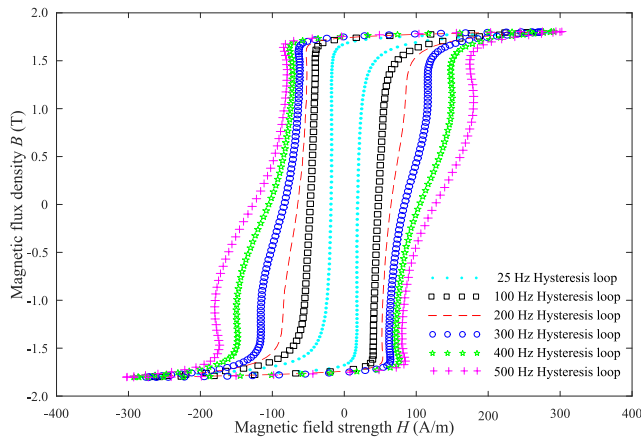


FIGURE 4. Hysteresis loops at different frequencies.

At the same time, we observe that the prediction accuracy of the neural network model for the remanence B_r is better than that for the coercivity H_c . In predicting coercivity, with the increase of frequency, the prediction error of the results obtained by neural network results decreases gradually. The higher the frequency value, the better the prediction accuracy of neural network. This can be attributed to the fact that the training data of the neural network have taken six frequency values of 25, 100, 200, 300, 400, and 500 Hz, as shown in Fig. 4. We observe from the Fig. 4 that, compared with the curves at 25 and 100 Hz, the side of hysteresis loop has obvious deformation since 200 Hz. Therefore, when the neural network was trained with hysteresis loop data with these characteristics, the information obtained from the curves at 200, 300, 400, and 500 Hz is more than that at 25 and 100 Hz. In the prediction, the prediction results are more in line with the curves at 200, 300, 400, and 500 Hz. Therefore, with the increase of frequency, the side deformation of the hysteresis loop increases, and the coercivity prediction of the hysteresis loop by the neural network becomes more accurate. However, as for the prediction of remanence, we observed that the prediction error of neural network is basically consistent. This is because the magnetic induction intensity selected in the experimental measurement is relatively large, which is 1.8T and close to the remanence value of the silicon steel sheet 30Q120 selected in the experiment. Therefore, the numerical difference of remanence at different frequencies are small.

Hence, when the neural network “learns” the hysteresis loop, the “information” obtained at different frequencies is basically the same, so the error of prediction results is approximate.

Based on the analysis of the experimental data, we can attribute the wide gap of the prediction results between coercivity and remanence to difference of coercivity greater than difference of remanence of hysteresis loops at different frequencies. Thus, the information obtained by the neural network during “learning” will differ greatly, and the results obtained in the prediction of coercivity will have a certain gap with the measured results. The top and bottom curves of the hysteresis loop almost coincide, and the remanence values are basically the same. The information obtained by the neural network from the training data are also consistent, and the prediction results are basically the same. Therefore, the remanence prediction error of the hysteresis loop with different frequencies is relatively small.

VII. CONCLUSION

The magnetization characteristics of 30q120 silicon steel sheet at different frequencies were measured by experiment, and the magnetic characteristic parameters of silicon steel sheet at different frequencies were obtained. The hysteresis model of ferromagnetic material considering the influence of frequency was established by using BP neural network, and the results were compared with the measured results, thus proving the accuracy of the neural network hysteresis model. The neural network model has different results for the prediction accuracy of B_r and H_c , the prediction result of B_r is better than that of H_c , and for the local change of hysteresis loops, the neural network hysteresis model can accurately achieve the prediction.

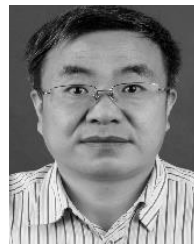
The commonly used dynamic J–A dynamic model is established, and the hysteresis loop at the corresponding frequency is calculated. After comparing it to the neural network hysteresis model, results show that the neural network model has higher accuracy.

According to the analysis of the prediction results, we find that the prediction error of the neural network model for coercivity shows a downward trend as the frequency increases. Thus, further expansion of the frequency range can be considered in the follow-up work. As there are many factors affecting the magnetization characteristics, only the

frequency factor is considered in this paper. The influence of DC bias, temperature, and other factors can be considered in the follow-up work.

REFERENCES

- [1] D. C. Jiles and D. L. Atherton, "Theory of ferromagnetic hysteresis," *J. Magn. Magn. Mater.*, vol. 61, nos. 1–2, pp. 48–60, Sep. 1986.
- [2] I. Mayergoz, "Mathematical models of hysteresis," *IEEE Trans. Magn.*, vol. MAG-22, no. 5, pp. 603–608, Sep. 1986.
- [3] S. Steentjes, K. Hameyer, D. Dolinar, and M. Petrun, "Iron-loss and magnetic hysteresis under arbitrary waveforms in NO electrical steel: A comparative study of hysteresis models," *IEEE Trans. Ind. Electron.*, vol. 64, no. 3, pp. 2511–2521, Mar. 2017, doi: [10.1109/TIE.2016.2570200](https://doi.org/10.1109/TIE.2016.2570200).
- [4] M. Petrun, S. Steentjes, K. Hameyer, and B. Polajzer, "Pragmatic modeling of dynamic magnetization and iron loss in grain-oriented steel sheets," *IEEE Trans. Magn.*, vol. 53, no. 11, pp. 1–5, Nov. 2017.
- [5] S. Piersanti, E. Pellegrino, G. Tresca, F. de Paulis, and A. Orlandi, "Equivalent circuit modeling in time domain of the hysteresis of magnetic materials," *IEEE Trans. Electromagn. Compat.*, vol. 57, no. 5, pp. 1013–1020, Oct. 2015.
- [6] K. Dezelak, M. Petrun, B. Klopčič, D. Dolinar, and G. Stumberger, "Usage of a simplified and Jiles–Atherton model when accounting for the hysteresis losses within a welding transformer," *IEEE Trans. Magn.*, vol. 50, no. 4, pp. 1–4, Apr. 2014.
- [7] M. Petrun, S. Steentjes, K. Hameyer, and D. Dolinar, "Analysis of different hysteresis models when considering magnetization dynamics in non-oriented soft magnetic steel sheet," in *Proc. IEEE Magn. Conf. (INTERMAG)*, May 2015, p. 1.
- [8] C. Li and Q. Xu, "Modeling of temperature dependent hysteresis based on Preisach theory," *Trans. China Electrotech. Soc.*, vol. 28, no. 12, pp. 90–94, Dec. 2013.
- [9] A. Raghunathan, Y. Melikhov, J. E. Snyder, and D. C. Jiles, "Modeling the temperature dependence of hysteresis based on Jiles–Atherton theory," *IEEE Trans. Magn.*, vol. 45, no. 10, pp. 3954–3957, Oct. 2009.
- [10] X. Zhao, X. Liu, F. Xiao, and Y. Liu, "Hysteretic and loss modeling of silicon steel sheet under the DC biased magnetization based on the Preisach model," *Trans. China Electrotech. Soc.*, vol. 35, no. 9, pp. 1849–1857, May 2020.
- [11] Z. Zhao, X. Ma, and J. Ji, "Simulation and experimental verification of magnetic characteristics of electrical steel sheet under DC bias based on energetic model," *Proc. The Chin. Soc. Electr. Eng.*, vol. 40, no. 14, pp. 4656–4665, Jul. 2020.
- [12] X. Xia, L. Wang, L. Shi, and M. Dong, "The magnetic properties of non-oriented electrical steel of different thickness under different frequency," *Anhui Metall.*, vol. 4, pp. 10–11, Dec. 2014.
- [13] G. Shi, Z. Liu, C. Li, P. Wang, and Q. Hu, "The magnetic research of non-oriented electrical steel in different frequency," in *Proc. 14th China Elect. Steel Annu. Conf.*, Zhejiang, China, Apr. 2017, pp. 228–231.
- [14] H. H. Saliyah, D. A. Lowther, and B. Forghani, "Modeling magnetic materials using artificial neural networks," *IEEE Trans. Magn.*, vol. 34, no. 5, pp. 3056–3059, Sep. 1998.
- [15] C. Serpico and C. Visone, "Magnetic hysteresis modeling via feed-forward neural networks," *IEEE Trans. Magn.*, vol. 34, no. 3, pp. 623–628, May 1998.
- [16] A. Laudani, G. M. Lozito, and F. R. Fulginei, "Dynamic hysteresis modelling of magnetic materials by using a neural network approach," in *Proc. AEIT Annu. Conf. From Res. Ind., Need More Effective Technol. Transf. (AEIT)*, Sep. 2014, pp. 1–6.
- [17] Z. Zhao, F. Liu, S. L. Ho, W. N. Fu, and W. Yan, "Modeling magnetic hysteresis under DC-biased magnetization using the neural network," *IEEE Trans. Magn.*, vol. 45, no. 10, pp. 3958–3961, Oct. 2009.
- [18] A. P. S. Baghel and S. V. Kulkarni, "Dynamic loss inclusion in the Jiles–Atherton (JA) hysteresis model using the original JA approach and the field separation approach," *IEEE Trans. Magn.*, vol. 50, no. 2, pp. 369–372, Feb. 2014.
- [19] H. Zhang, M. Tian, and P. D. Jing Wang, "Calculation and Analysis of Losses of magnetic-valve controllable reactor," *J. Meas. Sci. Instrum.*, vol. 11, no. 01, pp. 54–62, Jan. 2020.
- [20] Y. Wu, Y. Fang, X. Ren, and H. Lu, "Back propagation neural networks based hysteresis modeling and compensation for a piezoelectric scanner," in *Proc. IEEE Int. Conf. Manipulation, Manuf. Meas. Nanosc. (3M-NANO)*, Jul. 2016, pp. 119–124.
- [21] H. Fu, H. Zhao, and Y. Wang, *Application Design of MATLAB Neural Network*. Beijing, China: China Machine Press, 2010, pp. 40–65.
- [22] X. Wang and W. Shi, "BP algorithm for fitting the excitation characteristic curve," *J. Xi'an Jiaotong Univ.*, vol. 32, no. 8, pp. 1–4, Aug. 1998.
- [23] F. Liu, H. Y. Chen, S. Liu, and W. L. Yan, "Modeling magnetic hysteresis using neural network," *J. Hebei Univ. Technol.*, vol. 30, no. 2, pp. 33–36, Apr. 2001.
- [24] A. Laudani, G. M. Lozito, and F. R. Fulginei, "Dynamic hysteresis modelling of magnetic materials by using a neural network approach," in *Proc. AEIT Annu. Conf. Res. Ind., Need More Effective Technol. Transf. (AEIT)*, Sep. 2014, pp. 1–6.
- [25] G. K. Mitri, A. J. Moses, N. Derebasi, and D. Fox, "A neural network-based tool for magnetic performance prediction of toroidal cores," *J. Magn. Magn. Mater.*, vols. 254–255, pp. 262–264, Jan. 2003.
- [26] Z. Yuan and G. Liu, "Identification of transformer core hysteresis loop model parameters," *Power Syst. Clean Energy*, vol. 26, no. 9, pp. 17–19, Sep. 2010.
- [27] Y. Wang and Z. Liu, "The forecasting method of core loss under DC bias based on the Jiles Atherton hysteresis theory," *Proc. CSEE*, vol. 37, no. 1, pp. 313–323, Nov. 2011.
- [28] T. Hilgert, L. Vandeveld, and J. Melkebeek, "Neural-network-based model for dynamic hysteresis in the magnetostriction of electrical steel under sinusoidal induction," *IEEE Trans. Magn.*, vol. 43, no. 8, pp. 3462–3466, Aug. 2007.
- [29] G. Li et al., "Networks in simulation of ferromagnetic elements' major hysteresis curve," *Power Syst. Technol.*, vol. 25, no. 12, pp. 18–21, Dec. 2001.
- [30] R. Fang, "Prediction of performances for silicone plate under non-sinusoidal voltage waveform," *Transformer*, vol. 41, no. 5, pp. 13–16, May 2004.
- [31] Z. Wang, Y. Zhang, Z. Ren, C.-S. Koh, and O. A. Mohammed, "Modeling of anisotropic magnetostriction under DC bias based on an optimized BP neural network," *IEEE Trans. Magn.*, vol. 56, no. 3, pp. 1–4, Mar. 2020.
- [32] Z. Zhao, "Engineering-oriented modeling of power transformers under de-biased magnetization," Ph.D. dissertation, School Elect. Eng., Hebei Techn. Univ., Tianjin, China, 2010.



MINGXING TIAN was born in Gansu, China, in 1968. He is currently a Professor with the School of Automation and Electrical Engineering, Lanzhou Jiaotong University. His main research interests include analysis and control of power quality in power systems, design and control of electrical machine and electric appliance, and power electronics technology and its application.



HONGCHEN LI was born in Weifang, Shandong, China, in 1997. He received the bachelor's degree in electrical engineering from the Hebei University of Engineering, China, in 2019. He is currently pursuing the master's degree in power system and automation with the School of Automation and Electrical Engineering, Lanzhou Jiaotong University. His research interest includes analysis of magnetization characteristics of ferromagnetic materials.



HUIYING ZHANG was born in Shangqiu, Henan, China, in 1980. She received the bachelor's degree in electrical engineering and the M.S. degree in control theory and control engineering from Henan Polytechnic University, China, in 2003 and 2008, respectively. She is currently pursuing the Ph.D. degree in rail transit automation with the School of Automation and Electrical Engineering, Lanzhou Jiaotong University. Her research interests include magnetization characteristics of magnetic saturation reactor and numerical analysis of operation characteristics.

• • •